iScience

Article

Enhances the activity of mordenite in DME carbonylation reaction by controlling the degree of dealumination

Graphical abstract

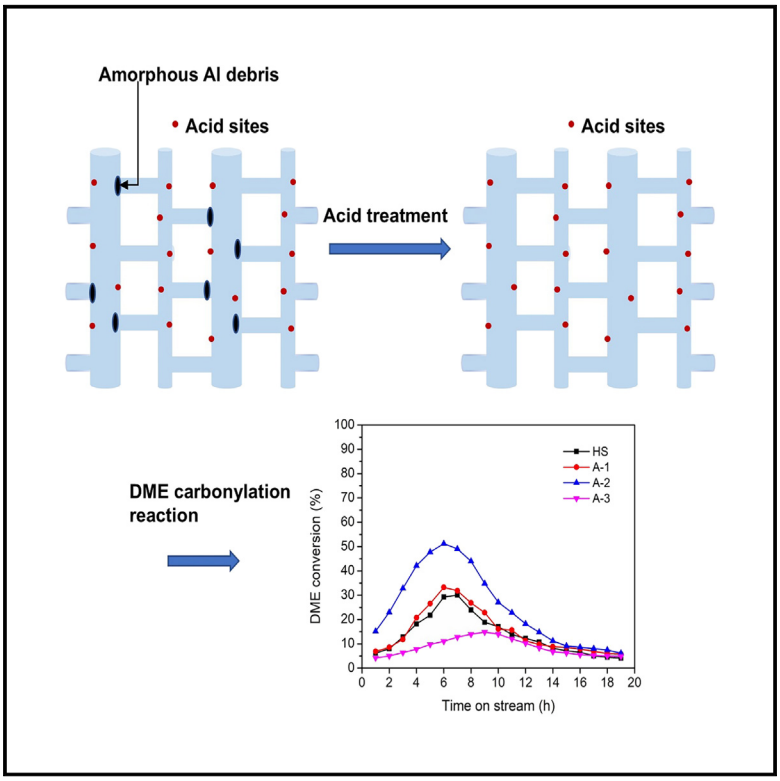

Highlights

- Degree of mordenite dealumination was controlled by mild acid treatment
- Available acid sites in side pocket of mordenite was increased by controlled dealumination
- Carbonylation activity of mordenite was improved with low degree of dealumination

Authors

Feng Xu, Junlin Zheng, Junhui Li, Zhirong Zhu

Correspondence

junhuili@tongji.edu.cn (J.L.), zhuzhirong@tongji.edu.cn (Z.Z.)

In brief

Chemical reaction; Catalysis; Materials characterization

Xu et al., 2025, iScience *28*, 112102
April 18, 2025
https://doi.org/10.1016/j.isci.2025.112102

CellPress

iScience

CellPress
OPEN ACCESS

Article

Enhances the activity of mordenite in DME carbonylation reaction by controlling the degree of dealumination

Feng Xu,[1,2] Junlin Zheng,[2] Junhui Li,[1,*] and Zhirong Zhu[1,3,*]
[1]School of Chemical Science and Engineering, Tongji University, Shanghai 200092, P.R. China
[2]Sinopec Shanghai Research Institute of Petrochemical Technology Co., Ltd., Shanghai 201208, P.R. China
[3]Lead contact
*Correspondence: junhuili@tongji.edu.cn (J.L.), zhuzhirong@tongji.edu.cn (Z.Z.)
https://doi.org/10.1016/j.isci.2025.112102

SUMMARY

A series of mordenites with different degree of dealumination were obtained by the acidic treatment and their catalytic properties in DME (dimethyl ether) carbonylation reaction were investigated. As a result, mild acid treated mordenite with low concentration can remove the extra-framework Al species only and open the side pocket, therefore increasing the amount of strong acid sites in it. Due to the increased accessibility of acid sites in the side pocket, the dealuminated mordenite showed a high catalytic activity in DME carbonylation reaction. Increasing the degree of dealumination of mordenite can preferentially destroy the framework Al atoms in side pocket. Therefore, the mordenite with severe dealumination exhibited a low activity in DME carbonylation reaction for reduced acid sites in the side pocket. Mild dealumination of mordenite can increase the catalytic activity in DME carbonylation reaction by 40% as compared to the parent mordenite in this work.

INTRODUCTION

The carbonylation of DME (dimethyl ether) over zeolite catalyst, provides an iodine-free method to synthesis MA (methyl estate), which is produced industrially as a byproduct in the process of methanol carbonylation.[1–5] This makes the route to synthesis ethanol from syngas environmentally and economically, as DME can be synthesis directly from syngas and MA can be hydrogenated to produce ethanol. All these reactions show excellent produce selectivity. The mechanism of DME carbonylation over acidic mordenite involves DME molecular adsorbed on Brønsted acid sites to form two methoxy groups, then carbon monoxide (CO) reacts with methoxy group to form an acylium cation, and DME molecular reacts with acylium cation to generate the methyl acetate.[4] CO attack on the methoxy group of mordenite to form an acylium cation intermediate is supposed to the rate determining step in the reaction.[6,7]

Mordenite exhibited the good catalytic performance in DME carbonylation reaction.[8–10] The framework of mordenite is composed of a series of parallel 12 MR (membered ring) channel and interconnected via small 8 MR channel which is perpendicular to the main channel.[11] The 12 MR channel of mordenite is responsible for catalyst deactivation, it showed a negligible carbonylation activity in the reaction but favored to formation of hydrocarbons through homologation and oligomerization reactions at higher temperature.[12] Quantum chemical study showed that the CO reacted with methoxy group occurs within 8 MR channel of mordenite, because the transition state formed on T3-O33 sites (within 8 MR channel) fit perfectly in the 8 MR channel, while large nucleophiles are sterically impeded.[6,7] The activation barrier of carbonylation on the T3-O33 sites was considerably lower than that for homologation and oligomerization reaction. The carbonylation rate increased with the increasing amount of acid sites in the 8-MR channel of mordenite.[13]

DME carbonylation reaction was often performed at the low temperature (150–220°C) to obtain high product selectivity, this also usually causes a relative low catalyst activity.[14–21] High-reaction temperature not only accelerates the carbonylation rate but also promotes the homologation and oligomerization reaction to form coke and results in catalyst deactivation. In order to improve catalytic activity of mordenite in DME carbonylation reaction, there are the strategies based on the two aspects: one is to enrich the acid sites in the side pocket of mordenite. Wang et al. reported that the acid sites distribution of mordenite was affected by the structure directing agent.[22] The acid sites in the 8 MR channels of mordenite was remarkably increased when using hexamethyleneimine as structure directing agent, and providing a high activity in the reaction. The Al content in gel also affects the acid sites distribution of as-synthesized mordenite. Wang et al. observed that Al atoms preferred to locate in the 8 MR channels of mordenite, and the acid sites distribution can be changed by gel composition.[23] The other one is increasing the accessibility of acid site in the side pocket. The size of 8 MR channels is too small and can be easily blocked by amorphous materials; this will hinder the mass diffusion and make the acid

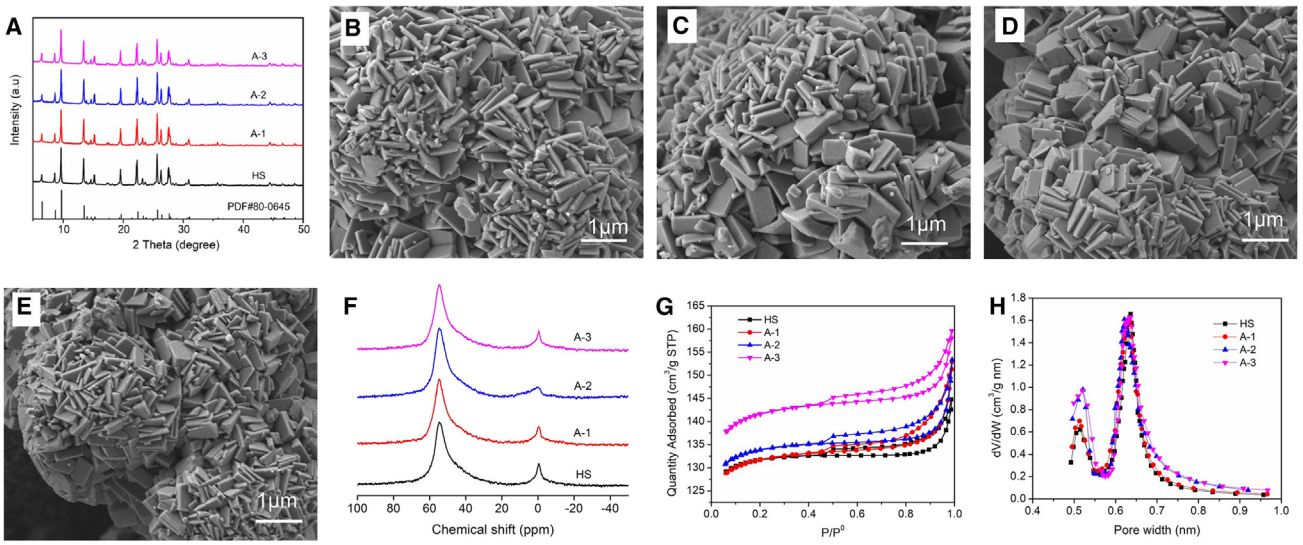

Figure 1. Structure and morphology of mordenite zeolites

(A) XRD patterns.

(B–E) SEM images of HS(B), A-1(C), A-2(D), and A-3(E) zeolites.

(F) ^{27}Al MAS NMR spectra.

(G) Ar adsorption and desorption isotherms.

(H) Pore-size distributions.

sites in the side pocket unavailable.[24,25] The amorphous species can be removed by means of post treatment, such as acid treatment or base treatment.[26–28]

Mordenite is an Al rich zeolite, acid treatment has been proved to be effective to improve its microporosity by dealumination.[25] However, severe dealumination of mordenite would cause an activity loss in the reaction.[27,29] The effect of acid treatment on zeolites is usually influenced by the factors, such as zeolite nature, solution concentration, treating time, and temperature.[25,30,31] In the present work, we investigated the optimum dealumination of mordenite and found that control the degree of dealumination of mordenite by acid treatment can improve the catalytic performance in the carbonylation of DME. This work may provide a method for developing high-performance zeolite catalyst for DME carbonylation.

RESULTS AND DISCUSSION

Textural properties of mordenite zeolites

The XRD (X-ray diffraction) spectra of all samples are shown in Figure 1A. It is found that mordenite samples kept MOR framework integrity after acid treatment. The intensity of the XRD reflections on 2 θ = 9.8°, 22.4°, 25.8°, and 26.4° was used to calculate the relative crystallinity of the samples, parent HS sample as a reference, the result was shown in Table 1.[32] Based on the XRD result, it was found that the concentration of hydrochloric acid solution affected the crystallinity of mordenite samples even on the low treatment temperature. The A-2 sample which treated in the low concentration of acid solution, exhibited a higher crystallinity than parent HS sample, due to the removal of amorphous Al species or Si species presented in the crystal. The crystallinity of A-3 sample was reduced to 86%, indicating partially damage to the zeolite framework, owing to a fact that part of framework Al atoms was extracted by severe acid treatment.

The content of sodium ions in all samples was less the 0.02 wt %. The bulk Si/Al ratio of parent HS sample was 8.1, the A-1 sample showed a similar value as HS sample. It was increased to 9.0 for A-2 sample and 10.6 for A-3 sample, respectively, as illustrated in Table 1. The variation in the value of Si/Al ratio confirmed the dealumination of mordenite during acid treatment, and the removal of Al species was remarkable in the high acid concentration. Scanning electron microscopy (SEM) images (Figures 1B–1E) showed that the parent HS sample had big crystals with the diameter of >10 μm, which was packed by numerous nanocrystals. Acid treatment seems to have negligible influence on the morphology of crystal in this experiment.

^{27}Al magic angle spinning nuclear magnetic resonance (^{27}Al MAS NMR) spectroscopy was used to investigate the coordination state of Al species existed in the mordenite, the result was recorded in Figure 1F. Two peaks at chemical shift of 55 ppm and 0 ppm were assigned to the framework Al and extra-framework Al, respectively.[33] The parent HS sample has a highest amount of Al_{ef} (extra-framework Al species, octahedral coordination), which was decreased with the acid treatment. As seen in the Table 1, the proportion of Al_{ef} was decreased from 14.8% for HS sample to12.4% for A-1 and 9.6% for A-2 sample, respectively, then increased to 11.6% for A-3 sample. Acid treated mordenite with low concentration seem to remove the extra-framework Al species more effectively. The small amount of Al_{ef} in A-2 sample suggested that most of extra-framework Al species were removed during the acid treatment. The extra-framework Al species in A-3 sample was higher than that in A-2 sample, due to the newly created extra-framework Al species which were generated from framework dealumination. As

Table 1. Physical-chemical properties of mordenite samples

Sample	Si/Al[a]	Crystallinity (%)	S_{BET} (m^2/g)	S_{micro} (m^2/g)	V_{micro} (cm^3/g)	V_{total} (cm^3/g)	Al_{ef}[b] (%)
HS	8.1	100	440	410	0.190	0.224	14.8
A-1	8.3	100	442	410	0.191	0.226	12.4
A-2	9.0	102	447	413	0.192	0.237	9.6
A-3	10.6	86	470	425	0.199	0.247	11.6

[a]The bulk Si/Al ratio is tested by ICP.
[b]The percentage of Al_{ef} is calculated by ^{27}Al MAS NMR.

a result, the degree of mordenite dealumination can be controlled by acid treatment. Mild acid treatment with low concentration favor to remove extra-framework Al species only, while severe acid treatment removes both the extra-framework Al and part of framework Al species.

The Ar adsorption-desorption isotherms are given in Figure 1G. All samples exhibited type IV isotherms with a hysteresis loop in the relative pressures that were higher than 0.4, indicating the presence of mesopore in the mordenite sample.[25] As observed in Table 1, acid treatment did not change the microporous structure, but enhanced the Ar uptake, specific surface area, and pore volume. The specific surface area of parent HS sample was 440 m^2/g, and it was increased to 447 m^2/g for A-2 sample and 470 m^2/g for A-3 sample, respectively. The specific surface area was increased with the degree of dealumination. Similar trend was also found in the pore volume of mordenite, the total pore volume increased from 0.224 cm^3/g for parent HS sample to the 0.237 cm^3/g for A-2 sample and 0.247 cm^3/g for A-3 sample. Amorphous Al species can occupy the zeolite channel and block the pores of 8-member channels, resulting in decreased pore volume and surface area.[34] Acid treatment can remove those amorphous material and clean the channel, therefore, increasing the specific surface area and pore volume of A-1 and A-2 sample, the result was confirmed by inductively coupled plasma optical emission spectroscopy (ICP) and ^{27}Al MAS NMR result. Severe acid treatment can extract the Al atoms from the framework, destroy the wall of channel, this may create the new pores and obtain the high specific surface area and pore volume. Figure 1H shows the curve of H-K pore size distribution, parent HS sample shows two peaks, the diameter of the pores in the range of <0.6 nm should be ascribed to the 8 MR channel, while the pores of 0.6–0.7 nm was the indicative of 12 MR channel.[35] After acid treatment, the height of peak in the range of <0.6 nm was significantly increased for A-2 and A-3 samples, and the peak at 0.6–0.7 nm for A-2 sample was broadened, indicating that pore volume of the small 8 MR channels were increased and the diameter of 12 MR channels were enlarged.

Acidic properties of mordenite samples

The acid properties of MOR zeolites were investigated by NH_3 temperature-programmed desorption (NH_3-TPD); the profiles were shown in Figure 2A. The desorption peak centered below 400°C was ascribed to weak and medium strong acids, while the peak centered above 400°C was ascribed to the strong acids, corresponding to the framework Al sites.[36,37] After acid treatment in the low concentration, the A-2 sample showed a lower peak in the low temperature range, and the peak in the high temperature range was increased significantly, as compared to the parent HS sample. It means that the amount of strong acid sites in A-2 sample was increased, the increased strong acid sites maybe from the acid sites located in the newly opened small 8 MR channels. When acid treatment in high concentration, the A-3 sample with a low desorption peak in the whole temperature range was obtained, indicating that the amount of acid sites in A-3 sample was dramatically decreased. The integration data were given in Table 2, the

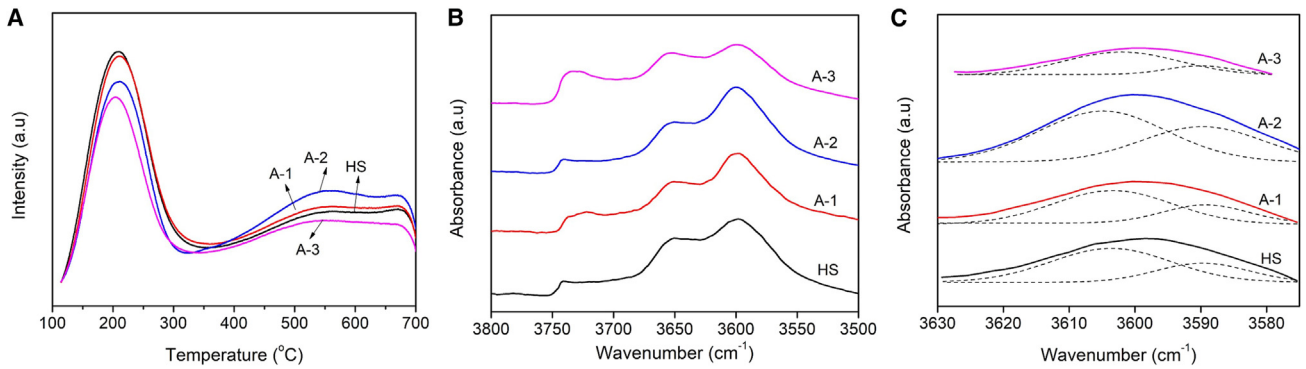

Figure 2. Acidity properties of mordenite zeolites
(A) NH_3-TPD.
(B) OH-IR spectra of 3,800–3,500 cm^{-1} region.
(C) Deconvoluted in 3,630–3,570 cm^{-1} region.

Table 2. Acidity properties of the mordenite samples

Sample	NH_3-TPD (mmol/g) Weak/Medium	Strong	Total	FTIR, B_{8MR}/B_{12MR}	B_{8MR}, (mmol/g)
HS	1.289	0.448	1.737	0.44	0.136
A-1	1.282	0.455	1.737	0.46	0.143
A-2	1.192	0.598	1.790	0.63	0.231
A-3	0.952	0.365	1.317	0.21	0.064

amount of weak and medium-strong acid sites of A-2 sample was 1.192 mmol/g, which was smaller than that of parent HS sample (1.289 mmol/g). The strong acid site of A-2 sample was 0.598 mmol/g, which was 1.33 times higher than that of parent HS sample. The amount of acid sites of A-3 sample was the lowest, the weak/medium-strong acid sites and strong acid sites was 0.952 mmol/g and 0.365 mmol/g, respectively.

The acid site distribution of Mordenite was determined by Fourier transform-infrared (FTIR) spectroscopy. The IR spectra with –OH stretching region between 3,500 cm^{-1} and 3,800 cm^{-1} were collected, as show in Figure 2B. A-1 sample showed similar spectra with parent HS sample at the band of 3,740 cm^{-1} and 3,650 cm^{-1}, which were associated with terminal Si groups and extra framework Al, respectively.[38,39] A significant increase at the band of 3,600 cm^{-1} associated with the framework Al atoms was observed on A-2 sample, suggesting the amount of Brønsted acid sites was increased. Compared to the parent HS sample, the A-3 sample showed a lower peak at the band of 3,600 cm^{-1}, which means the amount of framework Al atoms was decreased, it was consistent with the result from NH_3-TPD. An increased peak of 3,740 cm^{-1} was observed on A-3 sample, due to an increase in the amount of silanol groups which was formed by dealumination.

The peak at 3,600 cm^{-1} was deconvoluted into two peaks (Figure 2C) and the result was listed in Table 2. Two peaks located at 3,590 cm^{-1} and 3,610 cm^{-1} were assigned to the Brønsted acid sites in the 8 MR channel and 12 MR channel, respectively.[6,40,41] Compared to the parent HS sample, The peak at 3,590 cm^{-1} was increased on A-2 sample but decreased on A-3 sample. The area ratio of the 8 MR and 12 MR Brønsted acid sites were given in Table 2, it was 0.44 for parent HS sample, 0.46 for A-1 sample, 0.63 for A-2 sample, and 0.21 for A-3 sample. From the result, it was known that the amount of Brønsted acid sites in 8 MR channel of mordenite was increased after acid treatment with low concentration, while severe acid treatment can decrease the Brønsted acid sites in 8 MR channel preferentially. Combing with NH_3-TPD result, the Brønsted acid sites in the 8 MR channel was calculated, it was 0.136 mmol/g for parent HS sample, 0.143 mmol/g for A-1 sample, 0.231 mmol/g for A-2 sample, and 0.064 mmol/g for A-3 sample. The amount of Brønsted acid sites in the 8 MR channel of A-2 sample was largest, suggested that mild acid treatment not only increase the accessibility of 8 MR channels but also do not disturb the acid sites in it.

According to the above characterization result, it was known that mild acid treatment of mordenite with low concentration, only removed the extra-framework Al species and most of framework Al species were intact. It can increase the accessibility of 8MR channels, and increased the total amount of Brønsted acid sites of mordenite. When acid treatment of mordenite with high concentration, both the extra-framework Al and framework Al were removed. The amount of acid sites was decreased, especially the strong acid sites in the 8MR channel.

DME carbonylation over the parent and acid-treated mordenite zeolites

The catalytic performance of mordenite catalysts in DME carbonylation reaction was shown in Figures 3A–3D. All catalysts show a typically reaction behavior of DME carbonylation over mordenite catalyst.[4,14,42,43] The DME conversion increased during the induction period, then reaching the maximum value and began to decline gradually. In the induction period, all acid sites were methylated by DME molecules; it was 6 h for A-1 sample and A-2 sample, which was the same as the parent HS sample. The A-3 sample exhibited a longest induction period of 8 h, possibly due to extra-framework Al species generation by dealumination deposit in the channel and increased the resistance of mass diffusion. Meanwhile, the selectivity to methyl acetate gradually increased during the induction period, and the amount of methanol which was generated in the reaction of DME with Brønsted acid sites was decreased. When methylation reaction completed, both the DME conversion and the selectivity to methyl acetate reached to the maximum value. The peak DME conversion of A-2 sample was 51%, which was 1.7 times higher than that of parent HS sample and was 3.4 times higher than that of A-3 sample. All catalysts showed an excellent selectivity (>99%) to the methyl acetate in this period, due to the side pocket channel in mordenite had the ultrahigh selectivity to synthesis methyl acetate.[6,13]

The yield of methyl acetate on A-2 sample was 1.82 $g_{MA}g_{cat}^{-1}$, which was much higher than that of parent HS sample (0.95 $g_{MA}g_{cat}^{-1}$) and A-3 sample (0.60 $g_{MA}g_{cat}^{-1}$), as listed in Table 3. The value of peak activity per the amount of Brønsted acid sites in the 8MR channel was calculated, it was the same for all samples, which indicates the carbonylation rate was proportional to the acid sites in the 8MR channels of mordenite, convinced the result of previous study.[29] Without regard to the mass diffusion, increasing the acid sites in the 8MR channels maybe the only way to improve the catalyst activity in DME carbonylation reaction. Although the lowest catalyst activity was observed on A-2 sample, its deactivation rate was decreased due to the low acid density and reduced rate of side reaction.[12,29] The catalytic result revealed that the degree of dealumination strongly affected the catalytic performance of the mordenite catalyst in DME carbonylation reaction. Mild acid treatment of mordenite with low concentration was beneficial to increase the available Brønsted acid sites of 8 MR channel and improve its catalytic activity. While severe dealumination of mordenite preferentially destroyed the Brønsted acid sites in 8 MR channel and resulted in a decreased activity in the reaction of DME carbonylation.

Conclusion

The degree of mordenite zeolite dealumination was controlled by acid treatment with different concentration. Acid treatment of mordenite with low concentration only removed the extra-framework

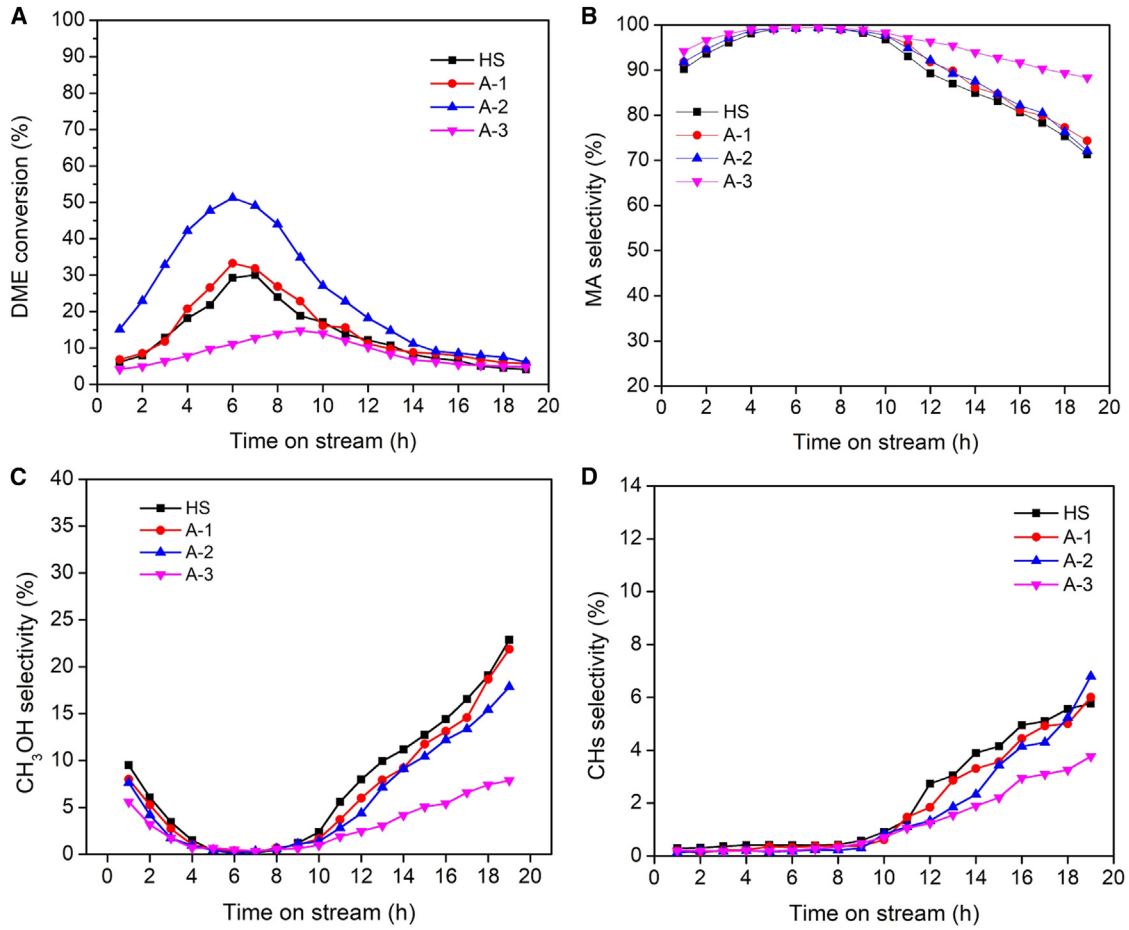

Figure 3. Catalytic performance for DME carbonylation reaction over mordenite zeolites

(A–D) DME conversion (A), selectivity to MA (B), CH_3OH (C), and CHs by-products (D) of HS, A-1, A-2, and A-3 samples as a function of reaction time. Reaction conditions: 473 K, 1.5 MPa, DME/CO = 1/40 (vol %), GHSV = 4,000 mL g^{-1} h^{-1}.

Al species, the accessibility of side pockets and the amount of strong acid sites of mordenite were increased, which resulted in a high catalytic activity for DME carbonylation reaction. While during a severe dealumination of mordenite treated by a high acid concentration, both the extra-framework Al species and framework Al species were removed, and the Brønsted acid sites in the side pocket were preferentially destroyed, causing a declined activity of mordenite in the DME carbonylation reaction. Therefore, a mild dealumination of mordenite by acid treatment is an effective way to improve the catalytic performance of mordenite in DME carbonylation.

Limitations of the study

This study provides a simple method to enhance the activity of mordenite in DME carbonylation. Further research will focus on the factors of acid treatment, such as acid types, treating time and temperature on the mordenite structure, and acidity using advanced characterization techniques.

RESOURCE AVAILABILITY

Lead contact

Further information and requests for resources should be directed to and will be fulfilled by the lead contact, Zhirong Zhu (zhuzhirong@tongji.edu.cn).

Table 3. Catalyst Performance in DME Carbonylation over mordenite catalysts

Sample	MA yield (g_{MA} g_{cat}^{-1})	Peak activity (g_{MA} $g_{cat}^{-1}h^{-1}$)	Peak activity per B_{8MR}[a] (g_{MA} $mmol^{-1}h^{-1}$)
HS	0.95	0.119	0.882
A-1	1.10	0.127	0.885
A-2	1.82	0.204	0.879
A-3	0.60	0.060	0.890

[a]The Peak activity per B_{8MR} = Peak activity/the value of B_{8MR}.

Materials availability

This study did not generate new unique reagents, and all reagents were commercially available and used without purification.

Data and code availability

- Data reported in this paper will be shared by the lead contact upon reasonable request.
- This paper does not report original code.
- Any additional information required to reanalyze the data reported in this paper is available from the lead contact upon request.

ACKNOWLEDGMENTS

The authors are grateful to the financial supports of the National Natural Science Foundation of China (no.91534115).

AUTHOR CONTRIBUTIONS

F.X., methodology and writing - original draft; J.Z. and J.L., writing – review and editing; Z.Z., supervision, data curation, funding acquisition, and reviewing.

DECLARATION OF INTERESTS

The authors declare no competing interests.

STAR★METHODS

Detailed methods are provided in the online version of this paper and include the following:

- KEY RESOURCES TABLE
- EXPERIMENTAL MODEL AND STUDY PARTICIPANT DETAILS
- METHOD DETAILS
  - Catalyst preparation
  - Characterization of catalyst
  - Catalysts test
- QUANTIFICATION AND STATISTICAL ANALYSIS
- ADDITIONAL RESOURCES

Received: December 17, 2024
Revised: January 24, 2025
Accepted: February 21, 2025
Published: February 25, 2025

REFERENCES

1. Sunley, G.J., and Watson, D.J. (2000). High productivity methanol carbonylation catalysis using iridium - The Cativa (TM) process for the manufacture of acetic acid. Catal. Today *58*, 293–307.
2. Fujimoto, K., Shikada, T., Omata, K., and Tominaga, H.O. (1984). Vapor phase carbonylation of methanol with solid acid catalyst. Chem. Lett. *13*, 2047–2050.
3. Cheung, P., Bhan, A., Sunley, G.J., and Iglesia, E. (2006). Selective carbonylation of dimethyl ether to methyl acetate catalyzed by acidic zeolites. Angew. Chem. Int. Ed. *45*, 1617–1620.
4. Cheung, P., Bhan, A., Sunley, G., Law, D., and Iglesia, E. (2007). Site requirements and elementary steps in dimethyl ether carbonylation catalyzed by acidic zeolites. J. Catal. *245*, 110–123.
5. Wegman, R.W. (1994). Vapour phase carbonylation of methanol or dimethyl ether with metal-ion exchanged heteropoly acid catalysts. J. Chem. Soc., Chem. Commun. *8*, 947–948.
6. Boronat, M., Martínez-Sánchez, C., Law, D., and Corma, A. (2008). Enzyme-like specificity in zeolites: A unique site position in mordenite for selective carbonylation of methanol and dimethyl ether with CO. J. Am. Chem. Soc. *130*, 16316–16323.
7. Boronat, M., Martinez, C., and Corma, A. (2011). Mechanistic differences between methanol and dimethyl ether carbonylation in side pockets and large channels of mordenite. Phys. Chem. Chem. Phys. *13*, 2603–2612.
8. Wang, S., Yin, S., Guo, W., Liu, Y., Zhu, L., and Wang, X. (2016). Influence of inlet gas composition on dimethyl ether carbonylation and the subsequent hydrogenation of methyl acetate in two-stage ethanol synthesis. New J. Chem. *40*, 6460–6466.
9. Liu, Y., Murata, K., Inaba, M., and Takahara, I. (2013). Synthesis of ethanol from methanol and syngas through an indirect route containing methanol dehydrogenation, DME carbonylation, and methyl acetate hydrogenolysis. Fuel Process. Technol. *110*, 206–213.
10. Volkova, G.G., Plyasova, L.M., Shkuratova, L.N., Budneva, A.A., Paukshtis, E.A., Timofeeva, M.N., and Likholobov, V.A. (2004). Solid superacids for halide-free carbonylation of dimethyl ether to methyl acetate. Stud. Surf. Sci. Catal. *147*, 403–408.
11. Simoncic, P., and Armbruster, T. (2004). Peculiarity and defect structure of the natural and synthetic zeolite mordenite: A single-crystal X-ray study. Am. Mineral. *89*, 421–431.
12. Li, B., Xu, J., Han, B., Wang, X., Qi, G., Zhang, Z., Wang, C., and Deng, F. (2013). Insight into Dimethyl Ether Carbonylation Reaction over Mordenite Zeolite from in-Situ Solid-State NMR Spectroscopy. J. Phys. Chem. C *117*, 5840–5847.
13. Bhan, A., Allian, A.D., Sunley, G.J., Law, D.J., and Iglesia, E. (2007). Specificity of sites within eight-membered ring zeolite channels for carbonylation of methyls to acetyls. J. Am. Chem. Soc. *129*, 4919–4924.
14. Xue, H., Huang, X., Ditzel, E., Zhan, E., Ma, M., and Shen, W. (2013). Coking on micrometer- and nanometer-sized mordenite during dimethyl ether carbonylation to methyl acetate. Chin. J. Catal. *34*, 1496–1503.
15. Liu, J., Xue, H., Huang, X., Li, Y., and Shen, W. (2010). Dimethyl ether carbonylation to methyl acetate over HZSM-35. Catal. Lett. *139*, 33–37.
16. Jung, H.S., Xuan, N.T., and Bae, J.W. (2021). Carbonylation of dimethyl ether on ferrierite zeolite: Effects of crystallinity to coke distribution and deactivation. Microporous Mesoporous Mater. *310*, 110669.
17. Wang, X., Li, R., Yu, C., Liu, Y., Xu, C., and Lu, C. (2021). Study on the deactivation process of dimethyl ether carbonylation reaction over Mordenite catalyst. Fuel *286*, 119480.
18. Reule, A.A., and Semagina, N. (2016). Zinc hinders deactivation of copper-mordenite: dimethyl ether carbonylation. ACS Catal. *6*, 4972–4975.
19. Guo, Y., Wang, S., Geng, R., Wang, P., Li, S., Dong, M., Qin, Z., Wang, J., and Fan, W. (2023). Enhancement of the dimethyl ether carbonylation activation via regulating acid sites distribution in FER zeolite framework. iScience *26*, 107748.
20. Tuo, J., Wang, J., Gong, X., Zhai, C., Xu, H., Xue, T., Jiang, J., Guan, Y., and Wu, P. (2024). Ferrierite nanosheets with preferential Al locations as catalysts for carbonylation of dimethyl ether. Fuel *357*, 130001.
21. Cao, K., Chen, W., Fan, D., Jia, Z., Chen, N., Zhu, D., Xu, S., Zheng, A., Tian, P., and Liu, Z. (2024). MOR nanosheets with tunable c-axis thickness and their catalytic performance in DME carbonylation. Chem. Eng. J. *487*, 150344.
22. Wang, M.X., Huang, S.Y., Lu, J., Cheng, Z.Z., Li, Y., Wang, S.P., and Ma, X.B. (2016). Modifying the acidity of H-MOR and its catalytic carbonylation of dimethyl ether. Chin. J. Catal. *37*, 1530–1538.
23. Wang, X., Li, R., Yu, C., Liu, Y., Liu, L., Xu, C., Zhou, H., and Lu, C. (2019). Influence of acid Site distribution on dimethyl Ether carbonylation over mordenite. Ind. Eng. Chem. Res. *58*, 18065–18072.
24. Nagano, J., Eguchi, T., Asanuma, T., Masui, H., Nakayama, H., Nakamura, N., and Derouane, E.G. (1999). 1H and 129Xe NMR investigation of the microporous structure of dealuminated H-mordenite probed by methane and xenon. Microporous Mesoporous Mater. *33*, 249–256.
25. Viswanadham, N., and Kumar, M. (2006). Effect of dealumination severity on the pore size distribution of mordenite. Microporous Mesoporous Mater. *92*, 31–37.

26. van Iaak, A.N.C., Gosselink, R.W., Sagala, S.L., Meeldijk, J.D., de Jongh, P.E., and de Jong, K.P. (2010). Alkaline treatment on commercially available aluminum rich mordenite. Appl. Catal. A-Gen. *382*, 65–72.

27. Wang, X., Li, R., Yu, C., Liu, Y., Zhang, L., Xu, C., and Zhou, H. (2019). Enhancing the dimethyl ether carbonylation performance over mordenite catalysts by simple alkaline treatment. Fuel *239*, 794–803.

28. Tsai, S.T., Chen, C.H., and Tsai, T.C. (2009). Base treated H-mordenite as stable catalyst in alkylbenzene transalkylation. Green Chem. *11*, 1349–1356.

29. Reule, A.A., Sawada, J.A., and Semagina, N. (2017). Effect of selective 4-membered ring dealumination on mordenite-catalyzed dimethyl ether carbonylation. J. Catal. *349*, 98–109.

30. ODonovan, A.W., OConnor, C.T., and Koch, K.R. (1995). Effect of acid and steam treatment of Na- and H-mordenite on their structural, acidic and catalytic properties. Microporous Mater. *5*, 185–202.

31. Ates, A., and Hardacre, C. (2012). The effect of various treatment conditions on natural zeolites: Ion exchange, acidic, thermal and steam treatments. J. Colloid Interface Sci. *372*, 130–140.

32. Hincapie, B.O., Garces, L.J., Zhang, Q., Sacco, A., and Suib, S.L. (2004). Synthesis of mordenite nanocrystals. Microporous Mesoporous Mater. *67*, 19–26.

33. Li, X., Prins, R., and van Bokhoven, J.A. (2009). Synthesis and characterization of mesoporous mordenite. J. Catal. *262*, 257–265.

34. Silaghi, M.C., Chizallet, C., Sauer, J., and Raybaud, P. (2016). Dealumination mechanisms of zeolites and extra-framework aluminum confinement. J. Catal. *339*, 242–255.

35. Ban, S., van Laak, A.N.C., Landers, J., Neimark, A.V., de Jongh, P.E., de Jong, K.P., and Vlugt, T.J.H. (2010). Insight into the effect of dealumination on mordenite using experimentally validated simulations. J. Phys. Chem. C *114*, 2056–2065.

36. Lonyi, F., and Valyon, J. (2001). On the interpretation of the NH3-TPD patterns of H-ZSM-5 and H-mordenite. Microporous Mesoporous Mater. *47*, 293–301.

37. Bagnasco, G. (1996). Improving the selectivity of NH3 TPD measurements. J. Catal. *159*, 249–252.

38. Groen, J., Sano, T., Moulijn, J., and Perez-Ramirez, J. (2007). Alkaline-mediated mesoporous mordenite zeolites for acid-catalyzed conversions. J. Catal. *251*, 21–27.

39. Paixao, V., Carvalho, A.P., Rocha, J., Fernandes, A., and Martins, A. (2010). Modification of MOR by desilication treatments: structural, textural and acidic characterization. Microporous Mesoporous Mater. *131*, 350–357.

40. Segawa, K., and Shimura, T. (2000). Effect of dealumination of mordenite by acid-leaching for selective synthesis of ethylenediamine from ethanolamine. Appl. Catal. A-Gen. *194–195*, 309–317.

41. Zhou, H., Zhu, W., Shi, L., Liu, H., Liu, S., Ni, Y., Liu, Y., He, Y., Xu, S., Li, L., and Liu, Z. (2016). In situ DRIFT study of dimethyl ether carbonylation to methyl acetate on H-mordenite. J. Mol. Catal. A: Chem. *417*, 1–9.

42. Ma, M., Huang, X., Zhan, E., Zhou, Y., Xue, H., and Shen, W. (2017). Synthesis of mordenite nanosheets with shortened channel lengths and enhanced catalytic activity. J. Mater.Chem. A. *5*, 8887–8891.

43. Liu, J., Xue, H., Huang, X., Wu, P.H., Huang, S.J., Liu, S.B., and Shen, W. (2010). Stability enhancement of H-mordenite in dimethyl ether carbonylation to methyl acetate by pre-adsorption of pyridine. Chin. J. Catal. *31*, 729–738.

STAR★METHODS

KEY RESOURCES TABLE

REAGENT or RESOURCE	SOURCE	IDENTIFIER
Chemicals, peptides, and recombinant proteins		
Ammonium nitrate	Sinopharm Chemical Reagent Co., Ltd	CAS:6484-52-2
Mordenite	Shanghai FUXU zeolite company	CAS:12445-20-4
Hydrochloric acid, 36∼38vol%	Sinopharm Chemical Reagent Co., Ltd	CAS:7647-01-0
CO, 99.99 vol%	Shanghai Shenkai Gases Technology Co., Ltd	CAS:630-08-0
Dimethyl ether, 99.99 vol%	Shanghai Shenkai Gases Technology Co., Ltd	CAS:115-10-6

EXPERIMENTAL MODEL AND STUDY PARTICIPANT DETAILS

This study does not use experimental models.

METHOD DETAILS

Catalyst preparation

Commercial mordenite zeolite of Si/Al=8∼10 was used as parent mordenite sample. The as-synthesized sample was firstly calcined in air at 550°C for 3 h to obtain Na-form mordenite. Then the Na-form mordenite was ion-exchanged with 1.0 mol/L NH_4NO_3 solution at 80°C for 4 h, followed by filtering and washing with deionized water. The procedure was repeated 3 times to ensure that all sodium ions were removed. The filtered solid was dried in an oven at 120°C for 10 h and followed by calcined at 500°C for 3 h, and the protonic-form parent mordenite was obtained (denoted as HS).

Acid treatment was carried out by adding Na-form mordenite power to the HCl solution with a weight ratio of 1/10. The mixture was stirred for 30 min at 40°C, followed by filtration and washing with deionized water until pH neutral. The obtained power was then ion-exchanged with NH_4NO_3 solution, and calcination in air to convert it into proton form, the procedure was the same as describe in above. In this process, the HCl solution of 0.02 mol/L, 0.1 mol/L and 0.5 mol/l were used, and the corresponding sample were denoted as A-1, A-2 and A-3.

Characterization of catalyst

XRD patterns were recorded by Bruker D8 advance power X-ray diffractometer using Cu K radiation, the scanning range is 5-40° with the speed of 5°/min. The composition of the sample was determined by an ICP-OES (Varian 725-ES), all samples were digest in HF aqueous solution for the test.

Ar adsorption-desorption isotherms experiments were conducted using micromeritics ASAP2020 at 77 K. Mordenite samples were degassed in vacuum at 350°C overnight. The specific surface areas were calculated through BET method using data between 0.001 and 0.1 P/P_0. The micropore pore size distribution and pore volume was obtained using the H-K method (Horvath-Kawazoe) .

NH_3-TPD (NH_3 temperature-programmed desorption) was obtained on micromeritics Autochem II 2920 instrument. The sample (100 mg) was placed in a quartz tube and pretreated in the He flow at 500°C for 1 h. After exposed to NH_3 gas for 30 min at room temperature, the sample was heated to 100°C in He flow to remove physiosorbed NH_3. Then the sample was heated to 700°C at a rate of 10°C/min, the desorbed NH_3 was monitored by thermal conductivity detector.

Scanning electron micrographs were taken with Philips Fei Quanta 200F. the samples were directly scanned without coating gold.

FT-IR (Fourier transform infrared spectra) were recorded in a Nicolet Nexus 470 infrared spectrometer combined with a homemade in-situ cell. The self-supported sample wafer was pretreated at 500°C for 1 h under vacuum. The FTIR spectra were collected at room temperature, in the range of 3400-3800 cm^{-1} with a resolution of 1cm^{-1}.

^{27}Al MAS NMR experiment were performed on a Bruker Advance III 600 spectrometer by using a 4 mm probe. The spectra were obtained with a reference to 1mol/L aqueous $Al(NO_3)_3$, the resonance frequency was 156.4 MHz and the spinning rate was kept at 14 kHz.

Catalysts test

DME carbonylation reaction were conducted in a continuous flow fixed-bed reactor. 1g of catalyst samples (20-40 mesh) were dehydrated in flowing N_2 for 2 h at 500°C, and cooled down to reaction temperature (200°C). The pressure of system was 1.5MPa and reactant mixture (DME / CO = 1/40, mol/mol) was introduced to the reactor through mass flowmeter, the GHSV was maintained constant at 4000 h^{-1}. The reactor effluent was transferred to an on-line gas chromatography system (Agilent 7890) through a

heated-traced lines (120°C), and the Agilent 7890 equipped with a Porapak Q packed column connected to flame ionization detector. The conversion of DME and selectivity to product was calculated on a molar basis from the chromatogram.

QUANTIFICATION AND STATISTICAL ANALYSIS

This study does not include statistical analysis or quantification.

ADDITIONAL RESOURCES

This study has not generated or contributed to a new website/forum and it is not part of a clinical trial.